

# Soft Actor-Critic with Backstepping-Pretrained DeepONet for control of PDEs

1<sup>st</sup> Chenchen Wang  
College of Information Science  
and Technology Donghua University  
Shanghai, China  
2242131@mail.dhu.edu.cn

2<sup>nd</sup> Jie Qi  
College of Information Science  
and Technology Donghua University  
Shanghai, China  
jieqi@dhu.edu.cn

3<sup>rd</sup> Jiaqi Hu  
College of Information Science  
and Technology Donghua University  
Shanghai, China  
hujiaqienjoy@gmail.com

**Abstract**—This paper develops a reinforcement learning-based controller for the stabilization of partial differential equation (PDE) systems. Within the soft actor-critic (SAC) framework, we embed a DeepONet, a well-known neural operator (NO), which is pretrained using the backstepping controller. The pretrained DeepONet captures the essential features of the backstepping controller and serves as a feature extractor, replacing the convolutional neural networks (CNNs) layers in the original actor and critic networks, and directly connects to the fully connected layers of the SAC architecture. We apply this novel backstepping and reinforcement learning integrated method to stabilize an unstable first-order hyperbolic PDE and an unstable reaction-diffusion PDE. Simulation results demonstrate that the proposed method outperforms the standard SAC, SAC with an untrained DeepONet, and the backstepping controller on both systems.

**Index Terms**—Reinforcement Learning, soft actor-critic, DeepONet, first-order hyperbolic PDEs, diffusion-reaction PDEs.

## I. INTRODUCTION

Control of PDE systems remains a highly challenging task due to the infinite-dimensional nature of the state space and the complexity of system dynamics. Learning-based approaches integrated with the classical control theory have emerged as a promising alternative, offering data-driven adaptability [1].

For finite-dimensional systems, there has been a growing body of research [2]–[4]. For instance, a control-informed reinforcement learning framework that integrates PID control components into the architecture of deep reinforcement learning (RL) policies is proposed in [5]. In this [6], it embeds barrier function theory into neural ordinary differential equations (ODEs), ensuring that the system state remains within a safe region by optimizing the parameters of a learning-based barrier function.

The infinite-dimensional nature of PDE systems poses significant challenges for control design, which has limited research progress in this field. For some special PDE systems there are some RL-based control design, such as applying proximal policy optimization to optimize the boundary controller for the Aw-Rasclé-Zhang (ARZ) model of highway traffic flow in [7]. Furthermore, by combining the state-dependent

Riccati equation (SDRE) with Bayesian linear regression, [8] proposes a RL-based algorithm for online identification and stable control of unknown PDEs.

However, one of the key challenges in combining classical control theory with learning-based methods lies in effectively incorporating prior knowledge from classical control into neural network learning. To address this issue, we propose a novel approach where a NO, specifically a Deep Operator Network (DeepONet) [9], [10], is pretrained to learn the backstepping controller, a well-established classical control law for PDE systems. DeepONet is particularly suited for this task as it can represent mappings from function spaces to function spaces, making it ideal for approximating the feedback operator. The use of DeepONet to learn backstepping gain functions/controllers is first proposed by [11], [12]. Subsequently, this approach is extended to handle PDE systems with delay [13]–[15], applied to enhance the real-time performance of adaptive control of PDEs [16], [17], and utilized in traffic flow control problems [18].

In our method, the DeepONet pretrained on the backstepping controller serves as a feature extractor, replacing the CNN layers in the standard SAC architecture. The DeepONet connects directly to the fully connected layers of the actor and critic networks. During training, the parameters of the DeepONet feature extractor are updated alongside the SAC actor and critic networks, enabling fine-tuning in the RL process.

The primary contribution of this paper is the introduction of a backstepping-pretrained DeepONet into the RL architecture. This accelerates training by providing better initialization, allowing the reward function to start from a higher baseline. We apply this novel backstepping and RL integrated method to stabilize an unstable first-order hyperbolic PDE and an unstable reaction-diffusion PDE. Simulation results show that the proposed method significantly reduces transient oscillations compared to the backstepping controller, vanilla SAC, and SAC with an untrained DeepONet. It also decreases the steady-state error relative to both SAC baseline algorithms. In our experiments, RL-based controllers exhibit small steady-state errors, likely due to the stochastic nature of their policies, whereas the rigorous backstepping controller can eliminate such errors. By integrating a pretrained DeepONet infused

The paper is supported by the National Natural Science Foundation of China (62173084), the Project of Science and Technology Commission of Shanghai Municipality, China (23ZR1401800).

Corresponding author: Jie Qi (jieqi@dhu.edu.cn)

with backstepping knowledge, the proposed method markedly reduces this error.

Additionally, when training the DeepONet, we incorporate not only state variables but also system coefficient functions as inputs. This design enables the pretrained DeepONet to adapt its output, the control effort, to variations in system coefficients. As a result, the trained RL controller remains effective even when applied to PDE systems with coefficients different from those seen during training, demonstrating the robustness of the method to parameter variations.

The structure of this paper is as follows: Section II provides problem formulation; Section III presents the NO-based reinforcement learning framework; Section IV validates the effectiveness of the method through simulations; and finally, Section V concludes the paper.

## II. PROBLEM DESCRIPTION

### A. General PDE control problem

We consider a one-dimensional PDE defined on a domain  $\mathcal{X} = [0, 1]$ . The time domain is  $\mathcal{T} = [0, T] \subset \mathbb{R}^+$ . Let  $u(x, t)$ , where  $x \in \mathcal{X}$  and  $t \in \mathcal{T}$ , describe the state of the system governed by the PDE, with the dynamics given by

$$\frac{\partial u}{\partial t} = F\left(u, \frac{\partial u}{\partial x}, \frac{\partial^2 u}{\partial x^2}, \dots, p_1(x), p_2(x), \dots, U(t)\right), \quad (1)$$

with the initial condition  $u(x, 0) = u_0(x)$ , where  $F$  is the PDE that models the system dynamics,  $U(t)$  is the control function, and  $p_i(x)$ , for  $i = 1, \dots, m$  are the coefficient functions with  $m$  coefficients. The PDE control problem is to design a controller which stabilize the system or a cost function regulates  $u(x, t)$  to a desired trajectory.

### B. Backstepping control operator

Employing the PDE backstepping method, one can design a feedback controller, usually the boundary controller, which is generalized by

$$U(t) = \int_0^1 k(x, y)u(y, t) dy, \quad (2)$$

where for given  $p_i(x) \in C[0, 1]$  and  $u \in C[0, 1]$ ,

$$U(t) := \mathcal{U}(p_1, \dots, p_m, u) = \int_0^1 k(x, y)u(y, t) dy, \quad (3)$$

with  $k(x, y)$  denoting the backstepping kernel function dependent on the system coefficients.

### C. DeepONet for learning backstepping controller

DeepONet is a deep learning architecture specifically designed for learning “function-to-function” mappings (operators). It consists of two subnetworks: a branch net and a trunk net. The output function is expressed as a weighted sum of basis functions, where the branch net learns the mapping from the input function to the coefficients (which serve as the weights of the basis functions), and the trunk net learns the basis functions themselves.

For the PDE control problem, the inputs to the DeepONet consist of the coefficients  $p_i(x)$  and state  $u(x, \cdot)$ , while the output of the DeepONet is the control signal  $U(\cdot)$ . All training data are generated by solving the PDE (1) with the backstepping controller (2), using different initial conditions and coefficient functions randomly sampled from Chebyshev polynomials with random parameters [11].

The trained DeepONet is adapted for integration into the SAC framework by modifying its output from a control value to a feature vector, as shown in Fig. 1. This feature vector serves as input to the FNN layers of both the actor and critic networks, introducing the backstepping control knowledge into the RL learning.

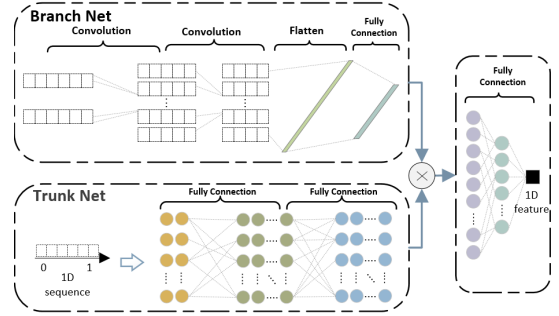


Fig. 1: Architecture of DeepONet as feature extractor for SAC.

## III. NO-BASED REINFORCEMENT LEARNING FRAMEWORK

In this section, we present the RL framework that integrates a pre-trained DeepONet with the SAC algorithm. We use a SAC framework with an actor network  $\pi_\phi(a_t|s_t)$ , two critic networks  $Q_{\theta_i}(s_t, a_t)$ , and their corresponding target networks  $Q_{\bar{\theta}_i}(s_t, a_t)$  (the dual-critic design mitigates bootstrapping issues). The DeepONet introduced in Section II-C, is pre-trained using the backstepping controller, which serves as a feature extractor and replaces the CNN layers in the standard SAC architecture. The DeepONet connects directly to the actor/critic fully connected layers. During training, the actor and critic networks, along with their embedded DeepONet feature extractors, are jointly trained via backpropagation. The architecture of the RL is shown in Fig. 2.

### A. Actor network

By introducing the policy entropy  $H_\pi$ , it measures the randomness of the action distribution given the state  $s_t$ . The policy entropy is defined as:  $H(\pi(\cdot|s_t)) = -\mathbb{E}_{a_t \sim \pi_\phi}[\log \pi_\phi(a_t|s_t)]$ . The policy network  $\pi_\phi(a_t|s_t)$  is trained by minimizing the following objective function:

$$J_\pi(\phi) = \mathbb{E}_{s_t \sim \mathcal{G}} \mathbb{E}_{a_t \sim \pi_\phi} \left[ -\alpha H(\pi_\phi(\cdot|s_t)) - \min_{i=1,2} Q_{\theta_i}(s_t, a_t) \right], \quad (4)$$

where  $\mathcal{G}$  denotes the state distribution. Accordingly, the parameter  $\phi$  of the policy network is updated by

$$\phi \leftarrow \phi - \eta \nabla_\phi J_\pi(\phi), \quad (5)$$

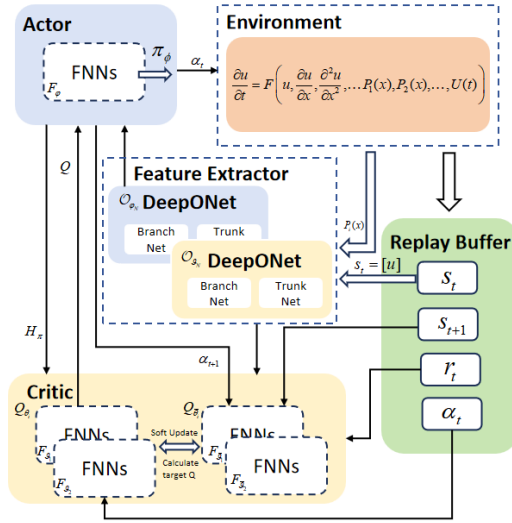


Fig. 2: The DeepONet pre-trained with the backstepping method is embedded into the SAC framework.

where  $\eta$  denotes the learning rate.

### B. Critic networks

We use a double Q-network structure (two independent FNNs), the action-value function is defined as  $Q_\pi(s_t, a_t)$ , which represents the expected cumulative return that the agent obtains by following the policy  $\pi_\phi$  after executing the action  $a_t$  in the state  $s_t$ . Using two target networks  $Q_{\bar{\theta}_{1,2}}$  to estimate the target action-value:

$$y_t = r_t + \gamma \left( \min_{i=1,2} Q_{\bar{\theta}_i}(s_{t+1}, \hat{a}_{t+1}) - \alpha \log \pi_\phi(\hat{a}_{t+1}|s_{t+1}) \right), \quad (6)$$

$\alpha$  is the temperature parameter, which is used to balance the trade-off between reward maximization and policy entropy, and the action  $\hat{a}_{t+1} \sim \pi(\cdot|s_{t+1})$  is sampled from the policy network. The weights of the target network  $Q_{\bar{\theta}_i}$  are updated by

$$\bar{\theta}_i \leftarrow \tau \theta_i + (1 - \tau) \bar{\theta}_i, \quad (7)$$

where  $i \in \{1, 2\}$  and  $\tau \in (0, 1]$  denotes the weighted coefficient.

The action-value networks  $Q_{\theta_1}(s_t, a_t)$  and  $Q_{\theta_2}(s_t, a_t)$  are trained by minimizing the following objective:

$$J_Q(\theta_i) = \mathbb{E}_{(s_t, a_t) \sim \mathcal{W}} [(Q_{\theta_i}(s_t, a_t) - y_t)^2], \quad (8)$$

where  $i \in \{1, 2\}$  and  $\mathcal{W}$  is the distribution of the states and actions. The parameter  $\theta_i$  is updated via stochastic gradient descent:

$$\theta_i \leftarrow \theta_i - \lambda \hat{\nabla}_{\theta_i} J_Q(\theta_i), \quad (9)$$

where  $\lambda$  denotes the learning rate.

### C. Algorithm (Markov Decision Process)

We have briefly outlined the processing of the Markov Decision Process (MDP), as shown in Algorithm 1.

1) State space  $\mathcal{S}$ : we denote  $s_t = \{u(x, t)\} \in \mathcal{S}$  as the augmented state at time  $t$ .

2) Action space  $\mathcal{A} \subseteq \mathbb{R}$ : it is defined as  $\mathcal{A} = [-\bar{U}, \bar{U}]$ , where  $\bar{U} = \sup_{t \in \mathbb{R}^+} |U(t)|$ ,  $U(t) = a_t \in \mathcal{A}$ .

3) Policy function  $\pi(a_t|s_t)$ : the policy is a probability density function  $\pi(a_t|s_t)$  that maps the current state  $s_t \in \mathcal{S}$  to a probability distribution over actions  $a_t \in \mathcal{A}$ .

4) State transition  $p(s_{t+1}|s_t, a_t)$ : this  $p(s_{t+1}|s_t, a_t)$  is the probability distribution of  $s_{t+1}$ , which depends on the current state  $s_t$  and the action  $a_t$  chosen by the agent. Given the state  $s_t$  at time  $t$ , when the agent executes action  $a_t$ , the environment transitions to the next state  $s_{t+1}$  following this probability distribution.

5) Reward function  $r_t$  and additional reward function  $q$ : it is designed to guide the learning of the optimal control policy. The reward function is defined as follows:

$$r_t(s_t, s_{t+1}) = -1 \cdot \|s_{t+1} - s_t\|_{L_2}, \quad (10)$$

$$q(s_T, a_0, \dots, a_T) = \begin{cases} 0 & \|s_T\|_{L_2} > \zeta, \\ \sigma - \frac{1}{\eta} \cdot \sum_{\tau=0}^T |a_\tau|_{L_1} & \|s_T\|_{L_2} \leq \zeta, \\ -\|s_t\|_{L_2} & \end{cases} \quad (11)$$

here,  $\sigma$ ,  $\eta$ , and  $\zeta$  are hyperparameters.

The reward function  $r_t$  is applied at each step to drive state convergence, while an additional reward  $q$  is given at the end of each episode if the  $L_2$  norm of the final state is less than or equal to a specified threshold  $\zeta$ .

---

#### Algorithm 1 SAC Procedure

---

- 1: Initialization:  $\phi, \theta_i, \bar{\theta}_i$  for  $i = 1, 2$ ,  $\mathcal{W}$  and  $s_0 = \{u_0(x)\}$
  - 2: **for**  $l \leftarrow 0$  to total steps **do**
  - 3:   **if**  $\|s_t\|_{L_2} > \text{limit} \vee t \geq T$  **then**
  - 4:     Reset initial state  $s_0$
  - 5:   **end if**
  - 6:   Observe current state  $s_t = \{u_t\}$
  - 7:   Sample action  $a_t \sim \pi_\phi(a_t | s_t)$
  - 8:   Execute  $a_t$ , observe  $s_{t+1}$  and  $r_t$
  - 9:    $\mathcal{W} \leftarrow \mathcal{W} \cup \{(s_t, a_t, r_t, s_{t+1})\}$
  - 10:   **for** each gradient step **do**
  - 11:     Sample a mini-batch from  $\mathcal{W}$
  - 12:     Compute the target value  $y_t$  using (6)
  - 13:     Update parameters of the  $Q_{\theta_{1,2}}$  by (8)
  - 14:     Update parameters of the  $Q_{\bar{\theta}_{1,2}}$  by (5)
  - 15:     Update parameters of the  $\pi_\phi$  by (4)
  - 16:   **end for**
  - 17: **end for**
- 

## IV. SIMULATION

In this section, we apply the proposed RL controller to both a hyperbolic PDE and a parabolic PDE. Details of the

corresponding backstepping designs can be found in [19]. The standard SAC code is obtained from the PDE Control Gym platform introduced in [20]. We compare our method (NOSAC\_training) with the backstepping controller (Backstepping), the standard SAC (SAC), and SAC embedded with DeepONet without pretraining the DeepONet using the backstepping controller (NOSAC).

Note that all the experiments are carried out on a workstation equipped with an Intel Core i9-13900KF CPU and an NVIDIA GeForce RTX 4090 GPU. For all the hyperparameters required by the SAC algorithm and the hyperparameters of the reward function, please refer to Appendix A.2 of [20].

### A. Simulation of a 1D Hyperbolic PDE

First, we train a DeepONet to approximate the backstepping controller. To generate the training data. We employ the finite difference method with a spatial step size of  $dx = 0.01$  over the time interval  $[0, 5]$  with a temporal step size of  $\Delta t = 0.001$ . The coefficient  $\beta(x)$  is sampled from the Chebyshev polynomial  $\beta(x) = 5 \cos(\gamma \cos^{-1}(x))$ , where  $\gamma \sim U[5.5, 7]$ . The initial condition  $u_0(x)$  is assumed to be a constant randomly chosen from the uniform distribution  $U[1, 10]$ .

We generate a dataset comprising  $6 \times 10^5$  samples, which were produced by combining 100 different  $\beta(x)$  and 60 different  $u_0(x)$ . During the data collection process, data was collected every 50 time steps. After completing the entire data collection, we randomly shuffled the dataset and split it into a training set 90% and a testing set 10%.

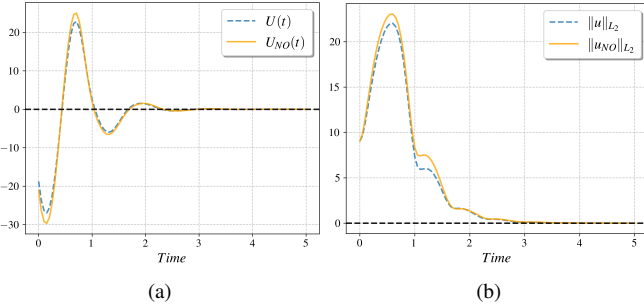


Fig. 3: (a) Control input and (b)  $L_2$  norm of the state  $u(x, t)$  for hyperbolic PDE with  $\gamma = 5.5$  and  $u_0(x) = 9$  under the backstepping controller and the DeepONet-approximated controller.

The DeepONet approximation results are shown in Fig. 3, illustrating the boundary control  $U(t)$  and the  $L_2$  norm of the state under the backstepping controller and the NO-based controller for  $\gamma = 5.5$ . It can be seen that the state converges to zero under both controllers.

The same  $\gamma$  value is used, and the initial state  $u_0(x)$  is randomly selected during RL. Training consists of 100,000 steps, with 100 interaction steps per episode. Fig. 4(a) shows the reward curves for SAC, NOSAC, and NOSAC\_training on 1D hyperbolic PDE, where NOSAC\_training achieves faster reward growth and finds effective policies more quickly than the other two.

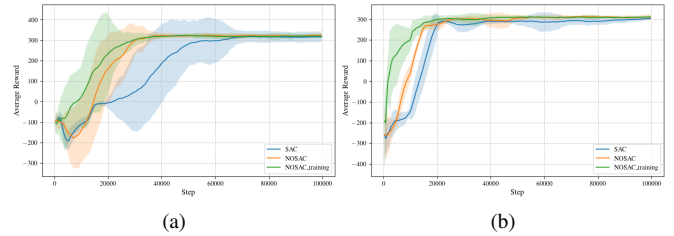


Fig. 4: Reward curves for the three RL training processes: (a) 1D Hyperbolic PDE, (b) 1D Parabolic PDE.

We apply the NOSAC\_training controller to the 1D hyperbolic PDE and compare its performance with the backstepping, SAC, and NOSAC, as shown in Fig. 5. The backstepping controller yields smoother closed-loop state evolution, while the proposed NOSAC\_training controller exhibits less overshoot. To better illustrate performance, Fig. 6 plots the control effort and the  $L_2$  norm of the state, showing that NOSAC\_training outperforms the backstepping controller, SAC, and NOSAC in terms of overshoot and convergence rate, while the backstepping controller achieves lower steady-state error.

To evaluate robustness under model mismatch, we simulate a system with  $\gamma = 5.7$  using the three LR-based controllers trained at  $\gamma = 5.5$  and the backstepping controller designed for  $\gamma = 5.5$ . The results in Fig. 6 demonstrate that NOSAC\_training achieves superior robustness, outperforming the other controllers in overshoot, convergence rate, and steady-state error.

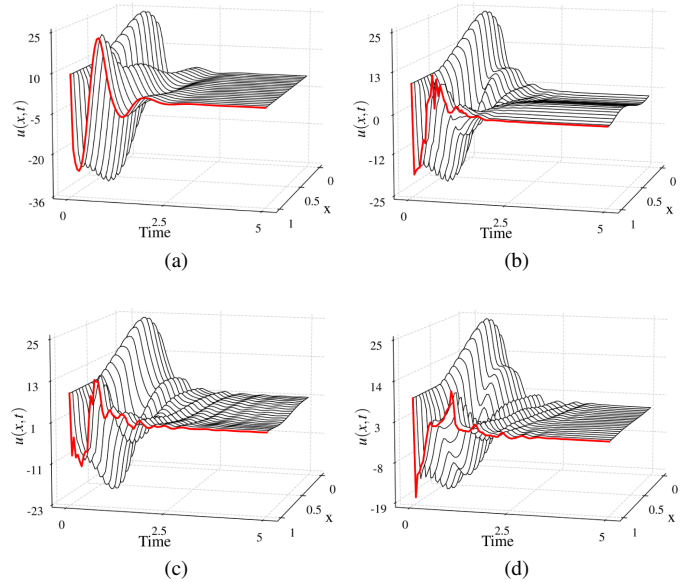


Fig. 5: Closed-loop state evolution with  $\gamma = 5.5$  and  $u_0(x) = 9$  under (a) Backstepping, (b) SAC, (c) NOSAC, (d) NOSAC\_training.

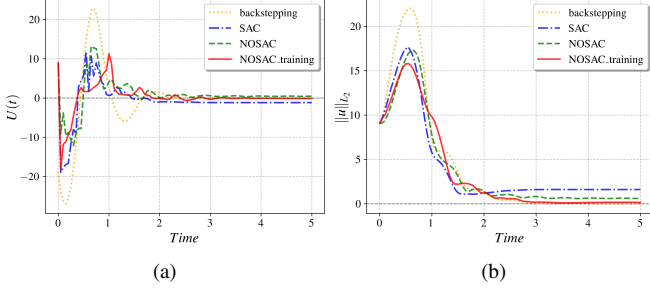


Fig. 6: (a) Control input and (b)  $L_2$  norm of the state with  $\gamma = 5.5$  and  $u_0(x) = 9$  under the four different controllers.

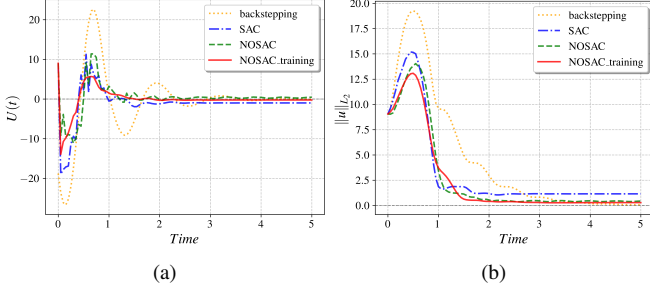


Fig. 7: (a) Control input and (b)  $L_2$  norm of the state under model mismatch with system's parameter  $\gamma = 5.7$  and initial condition  $u_0(x) = 9$  while training the three RLs and designing the backstepping using  $\gamma = 5.5$ .

### B. Simulation of a 1D Parabolic PDE

When dealing with 1D Parabolic PDE, the implicit method is employed, which enhances accuracy and reduces computation. We employ the  $dx = 0.01$  over the time interval  $[0, 1]$  with a temporal step size of  $\Delta t = 0.001$ . The coefficient  $\lambda(x)$  is sampled from the Chebyshev polynomial  $\lambda(x) = 50 \cos(\gamma \cos^{-1}(x))$ , where  $\gamma \sim U[8, 12]$ . We generate a dataset comprising  $6 \times 10^5$  samples, which were produced by combining 100 different  $\lambda(x)$  and 60 different  $u_0(x)$ . During the data collection process, data was collected every 100 time steps, its DeepONet training process is the same as that for the 1D Hyperbolic PDE. During testing, we extend the time  $T$  to 3 seconds to observe the effects.

The DeepONet approximation results are shown in Fig. 8, illustrating the boundary control  $U(t)$  and the  $L_2$  norm of the state under the backstepping controller and the NO-based controller for  $\gamma = 9$ . It can be seen that the state converges to zero under both controllers.

The same  $\gamma$  value is used, and the initial state  $u_0(x)$  is randomly selected during the RL, the RL training process is the same as that for 1D Hyperbolic PDE. Fig. 4(b) shows the reward curves for SAC, NOSAC, and NOSAC\_training on 1D Parabolic PDE, where NOSAC\_training achieves faster reward growth.

We apply the NOSAC\_training controller to the 1D parabolic PDE and compare its performance with the backstep-

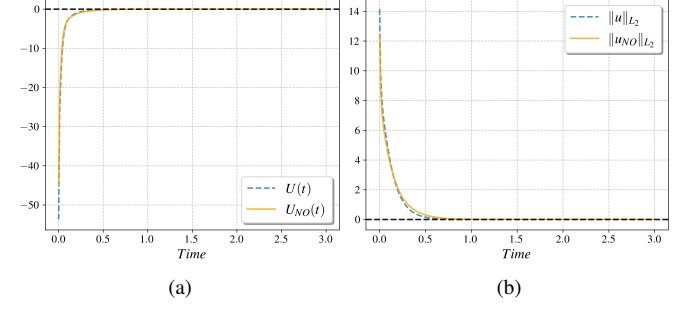


Fig. 8: (a) Control input and (b)  $L_2$  norm of the state  $u(x, t)$  for hyperbolic PDE with  $\gamma = 9$  and  $u_0(x) = 9$  under the backstepping controller and the DeepONet-approximated controller.

ping, SAC, and NOSAC, as shown in Fig. 9. The proposed NOSAC\_training controller exhibits less overshoot. Fig. 10 plots the control effort and the  $L_2$  norm of the state, showing that NOSAC\_training is optimal in terms of overshoot and convergence speed, while the backstepping controller achieves a lower steady-state error.

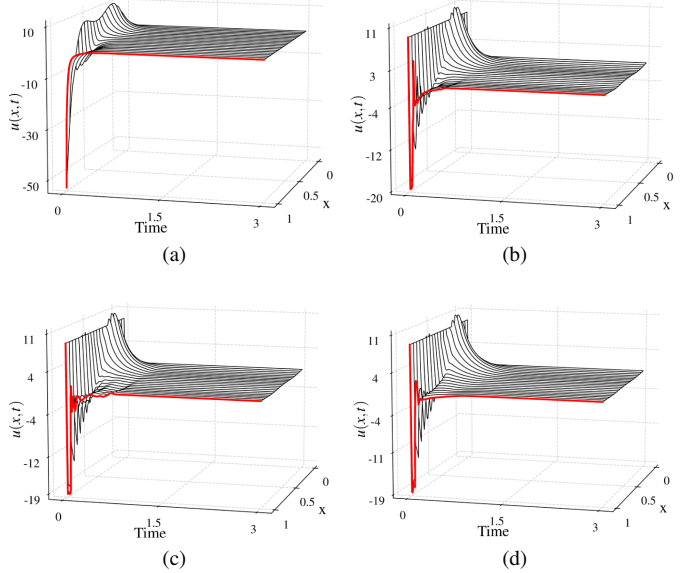


Fig. 9: Closed-loop state evolution with  $\gamma = 9$  and  $u_0(x) = 9$  under (a) Backstepping, (b) SAC, (c) NOSAC, (d) NOSAC\_training.

To evaluate robustness under model mismatch, we simulate a system with  $\gamma = 8.5$  using the three LR-based controllers trained at  $\gamma = 9$  and the backstepping controller designed for  $\gamma = 9$ . The results in Fig. 11 demonstrate that NOSAC\_training achieves superior robustness, outperforming the other controllers in overshoot, convergence rate, and steady-state error. Note that the backstepping controller performs worse for the parabolic PDE than the hyperbolic PDE under model mismatch.

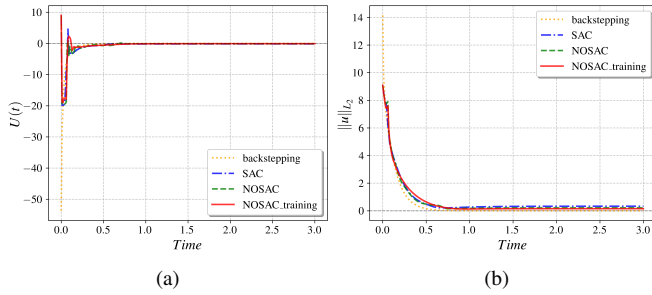


Fig. 10: (a) Control input and (b)  $L_2$  norm of the state with  $\gamma = 9$  and  $u_0(x) = 9$  under the four different controllers.

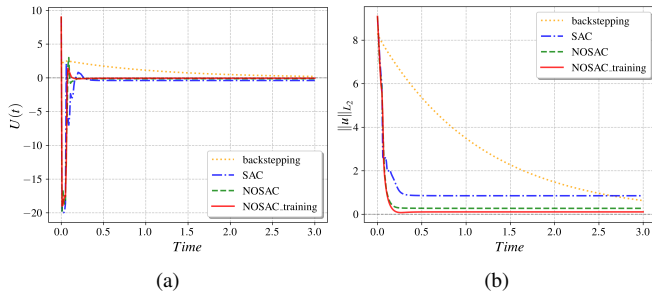


Fig. 11: (a) Control input and (b)  $L_2$  norm of the state under model mismatch with system's parameter  $\gamma = 8.5$  and initial condition  $u_0(x) = 9$  while training the three RLs and designing the backstepping using  $\gamma = 9$ .

## V. CONCLUSION

This paper develops a novel neural-operator-embedded SAC architecture for PDE control, which incorporates the knowledge of rigorous control through a DeepONet that approximates the backstepping controller. We apply this learning-based control methodology to both a 1D hyperbolic and a 1D parabolic unstable PDE, and evaluate its performance in terms of overshoot, convergence rate, and steady-state error, compared to the backstepping controller, standard SAC, and SAC embedded with a non-pretrained DeepONet. Simulations on both systems demonstrate that the proposed method outperforms the other three controllers. The robustness against model mismatch is also evaluated by changing the system coefficient to a value different from that used for control design. The results show that the proposed method achieves superior performance compared to the other approaches, owing to the pre-trained DeepONet's ability to adapt to varying coefficient functions and generate appropriate control signals in response to these changes. Future research will explore integrating safety control with this learning-based approach.

## REFERENCES

[1] T. Quartz, R. Zhou, H. De Sterck, and J. Liu, "Stochastic reinforcement learning with stability guarantees for control of unknown nonlinear systems," *arXiv preprint,2409.08382*, 2024.

[2] I. D. J. Rodriguez, A. Ames, and Y. Yue, "Lyanet: A Lyapunov framework for training neural ODEs," in *International Conference on Machine Learning (ICML)*, ser. Proceedings of Machine Learning Research, vol. 162. PMLR, 2022, pp. 18 687–18 703.

[3] J. H. S. Ip, G. Makrygiorgos, and A. Mesbah, "Lyapunov neural ODE feedback control policies," *arXiv preprint,2409.00393*, 2024.

[4] F. Berkenkamp, M. Turchetta, A. P. Schoellig, and A. Krause, "Safe model-based reinforcement learning with stability guarantees," in *Advances in Neural Information Processing Systems 30 (NeurIPS 2017)*, Long Beach, CA, USA, 2017, pp. 4480–4490.

[5] M. Bloor, A. Ahmed, N. Kotecha *et al.*, "Control-informed reinforcement learning for chemical processes," *Industrial & Engineering Chemistry Research*, vol. 64, no. 9, pp. 4966–4978, 2025.

[6] R. Yang, R. Jia, X. Zhang, and M. Jin, "Certifiably robust neural ODE with learning-based barrier function," *IEEE Control Systems Letters*, vol. 7, pp. 1634–1639, 2023.

[7] H. Yu *et al.*, "Reinforcement learning versus PDE backstepping and PI control for congested freeway traffic," *IEEE Transactions on Control Systems Technology*, vol. 30, no. 4, pp. 1595–1611, 2021.

[8] A. Alla, A. Pacifico, M. Palladino *et al.*, "Online identification and control of PDEs via reinforcement learning methods," *Advances in Computational Mathematics*, vol. 50, no. 4, p. 85, 2024.

[9] L. Lu, P. Jin, G. Pang *et al.*, "Learning nonlinear operators via deepnet based on the universal approximation theorem of operators," *Nature machine intelligence*, vol. 3, no. 3, pp. 218–229, 2021.

[10] H. Hu and C. Liu, "On the boundary feasibility for PDE control with neural operators," *arXiv preprint,2411.15643*, 2024.

[11] L. Bhan, Y. Shi, and M. Krstic, "Neural operators for bypassing gain and control computations in PDE backstepping," *IEEE Transactions on Automatic Control*, vol. 69, no. 8, pp. 5310–5325, 2023.

[12] M. Krstic, L. Bhan, and Y. Shi, "Neural operators of backstepping controller and observer gain functions for reaction–diffusion PDEs," *Automatica*, vol. 164, p. 111649, 2024.

[13] J. Qi, J. Hu, J. Zhang, and M. Krstic, "Neural operator feedback for a first-order PIDE with spatially-varying state delay," *arXiv preprint,2412.08219*, 2024.

[14] J. Qi, J. Zhang, and M. Krstic, "Neural operators for PDE backstepping control of first-order hyperbolic PIDE with recycle and delay," *Systems & Control Letters*, vol. 185, p. 105714, 2024.

[15] S. Wang, M. Diagne, and M. Krstic, "Deep learning of delay-compensated backsteps for reaction-diffusion PDEs," *IEEE Transactions on Automatic Control*, 2025.

[16] M. Lamarque, L. Bhan, Y. Shi *et al.*, "Adaptive neural-operator backstepping control of a benchmark hyperbolic PDE," *Automatica*, vol. 177, p. 112329, 2025.

[17] L. Bhan, Y. Shi, and M. Krstic, "Adaptive control of reaction–diffusion PDEs via neural operator-approximated gain kernels," *Systems & Control Letters*, vol. 195, p. 105968, 2025.

[18] C. Zhao and H. Yu, "Observer-informed deep learning for traffic state estimation with boundary sensing," *IEEE Transactions on Intelligent Transportation Systems*, vol. 25, no. 2, pp. 1602–1611, 2023.

[19] M. Krstic and A. Smyshlyaev, *Boundary control of PDEs: A course on backstepping designs*. Society for Industrial and Applied Mathematics, 2008.

[20] L. Bhan, Y. Bian, M. Krstic *et al.*, "PDE control gym: A benchmark for data-driven boundary control of partial differential equations," in *Proceedings of Machine Learning Research*, vol. 242. PMLR, 2024, pp. 1–26.